Chemical Vapor Deposition

The Mechanism of Chemical Vapor Deposition of Cubic Boron Nitride Films from Fluorine-Containing Species**

W. J. Zhang, C. Y. Chan, X. M. Meng, M. K. Fung, I. Bello, Y. Lifshitz, S. T. Lee, and X. Jiang*

The unique properties of cubic boron nitride (cBN) make it an excellent material for mechanical and electronic applications. Powders of cBN were synthesized by using a high-pressure, high-temperature method[1] and films of cBN were deposited by energetic ion-assisted physical vapor deposition (PVD).[2–5] The latter technique involves two distinct stages: nucleation and growth. The nucleation of cBN is preceded by a soft incubation interlayer of, first, amorphous BN (aBN) and, second, turbostratic BN (tBN). cBN nucleates on the edges of the basal planes of tBN. Energetic particle bombardment is crucial to cBN nucleation but results in highly stressed, nanocrystalline cBN films with poor adhesion and a limited thickness, thus hindering both mechanical and electronic applications. Deposition through energetic particle bombardment is a shallow implantation ("subplantation") process,[6] that is, nucleation and growth occur at several atomic layers below the surface.[7] This process is the origin of the sp^2-bonded aBN/tBN top surface layer that covers the cBN crystallites in PVD cBN films.

[*] Dr. W. J. Zhang,[+] C. Y. Chan, X. M. Meng,[+] Dr. M. K. Fung, Dr. I. Bello, Prof. S. T. Lee[+]
Center Of Super-Diamond and Advanced Films (COSDAF) and Department of Physics and Materials Science
City University of Hong Kong
Kowloon, Hong Kong SAR (China)
Fax: (+852) 2788-7830
E-mail: apwjzh@cityu.edu.hk

Prof. Y. Lifshitz
Center Of Super-Diamond and Advanced Films (COSDAF) and Department of Physics and Materials Science
City University of Hong Kong
Kowloon, Hong Kong SAR (China)
and
Department of Materials Engineering, Technion
Israel Institute of Technology
Haifa 32000 (Israel)

Prof. X. Jiang
Institute of Materials Engineering
University of Siegen
Paul-Bonatz-Strasse 9–11, 57076 Siegen (Germany)

[+] Additional address:
Nano-Organic Photoelectronic Laboratory
Technical Institute of Physics and Chemistry
The Chinese Academy of Science
Beijing 100101 (China)

[**] This work was supported by the Research Grants Council of the Hong Kong Special Administrative Region, China (Project Nos. CityU 1131/04E and CityU 1130/04E). W.J.Z. acknowledges the Alexander von Humboldt Foundation for supporting the collaboration between the City University of Hong Kong and the University of Siegen.

 DOI: 10.1002/ange.200500320

Chemical vapor deposition (CVD) of diamond employs hydrogen chemistry to selectively etch sp^2-bonded carbon atoms to grow high-quality, thick films. Hydrogen does not selectively etch sp^2-bonded BN, thus attempts to grow cBN by hydrogen-based CVD methods failed.[8] However, the deposition of films of up to around 20-μm thick of cBN by fluorine-based bias-assisted CVD methods was recently reported.[9–11] Similar to the CVD of diamond, the nucleation stage of cBN requires an ion-assisted physical mechanism that involves a tBN incubation interlayer as described previously.[10] The application of fluorine-containing species for the growth stage that follows this nucleation enables a drastic decrease in the required bombarding ion energy (< 20 eV),[11] especially for the direct deposition of cBN on diamond, upon which no interlayer (no nucleation stage) forms.[12]

Herein, we show the successful development of a surface CVD growth process of cBN and outline a new mechanism initiated by the introduction of fluorine-containing species. Our study involves a combination of high-resolution transmission electron microscopy (HR-TEM) characterization of the topmost layers of cBN films, X-ray photoelectron spectroscopy (XPS) analysis of the composition of the surface of the film, and optical emission spectroscopy (OES) of the composition of the plasma. The possibility of growing cBN by a true surface CVD process and the understanding of the growth mechanism paves the way to the growth of single-crystal, electronic-grade wafers of cBN for electronic applications.

Deposition of the cBN film was performed in an electron cyclotron resonance (ECR)-enhanced microwave (MW) plasma of a $He(Ar)/N_2/BF_3/H_2$ gas mixture generated by an ASTeX 1.5 kW MW source with a magnetic field of approximately 875 G.[13] The deposition conditions were as follows: MW power, 1.4 kW; pressure, 2×10^{-3} Torr; Ar and He (plasma-processing gases) flow, 10 and 140 std $cm^3 min^{-1}$, respectively; N_2, BF_3, and H_2 (reactant gases) flow, 50, 1.5, and 3 std $cm^3 min^{-1}$, respectively. During deposition, a bias voltage of -20 to -40 V was applied to the substrate, which was maintained at about 950 °C as measured by an optical pyrometer.

We first discuss a comparative HR-TEM study of the structure of the topmost layers of two samples, A (deposited by CVD) and B (deposited by bias-enhanced radio-frequency magnetron sputtering PVD[14]). Both samples were coated with a protecting layer of gold (10-nm thick) directly after deposition of cBN. Specimens for cross-sectional TEM were prepared by the standard procedure, that is, grinding, dimpling, and final ion milling. A 200 kV field-emission TEM apparatus (Philips CM200) was used.

Figure 1 displays cross-sectional overviews of samples A (Figure 1a) and B (Figure 1b). Figure 1a (CVD sample) shows a clear interface between the cBN film and the gold layer and that the cBN and gold lattices are in direct contact; there is no amorphous interlayer. Figure 1b (PVD sample) shows a much more defective, nanocrystalline cBN structure with aBN and tBN impurities and a thin aBN top layer (indicated) that clearly covers the surface of the cBN film with a thickness of about three atomic layers.

A layer of aBN is absent from the top of the CVD cBN film, yet it is present on the film obtained by PVD. This

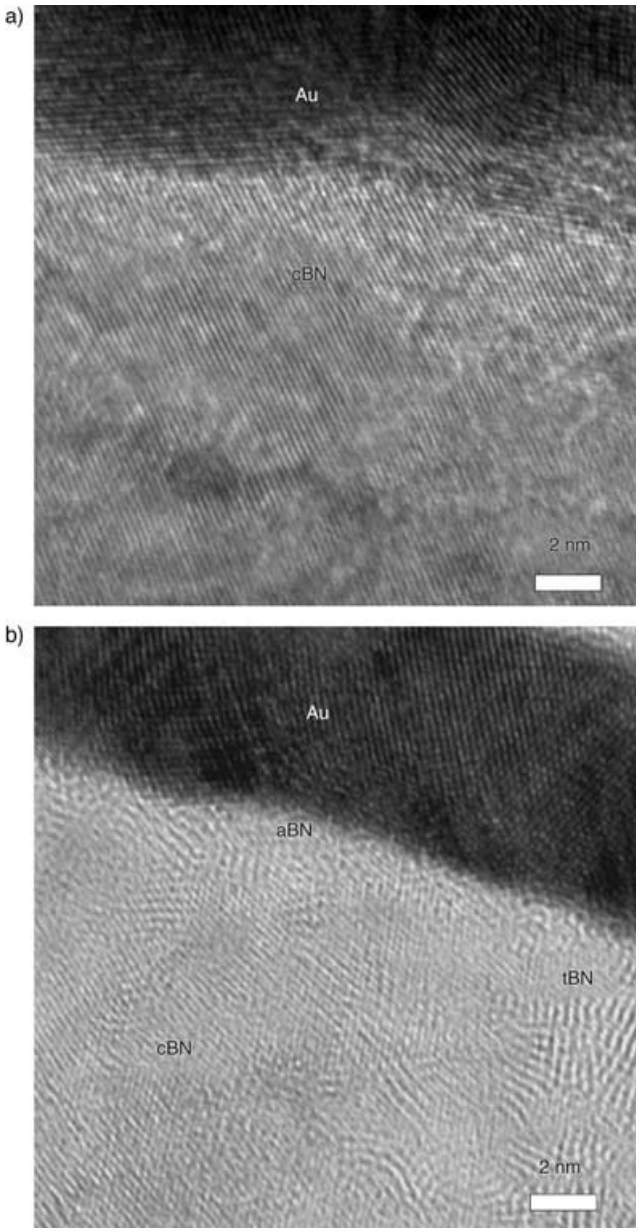

Figure 1. Cross-sectional HR-TEM image of the surface region of the film deposited by a) ECR MW CVD and b) magnetron sputtering. A gold coating on the cBN surface protects and marks the surface region.

indicates the difference between the growth mechanisms in the two deposition schemes: CVD involves a surface-growth process associated with surface etching, whereas PVD involves a subsurface growth that leads to a typical aBN skin. In accord with the TEM data, SEM images (not shown) indeed show the faceted nature of the CVD films[15] which is not observed for the PVD films. The HR-TEM data thus substantiate the conclusion that cBN growth by chemical pathways was obtained by the introduction of fluorine-containing species.

Optical emission spectroscopy of the plasma used for cBN growth reveals the reactive gas species and provides insight into the growth mechanism. The small quantity of BF_3 and H_2

used relative to the much larger amounts of Ar, He, and N_2 present inhibit the observation of most reactant species in the actual plasma used for cBN growth. Hence, we chose to study the composition of the $BF_3 + H_2$ plasma with different H_2/BF_3 ratios (0:1 to 5:1) instead. The study was performed by using a substrate holder made of hBN to enable the observation of hBN etching by $BF_3 + H_2$ plasma. OES of pure BF_3 plasma (Figure 2a) indicates the formation of atomic F, BF, H, and N_2

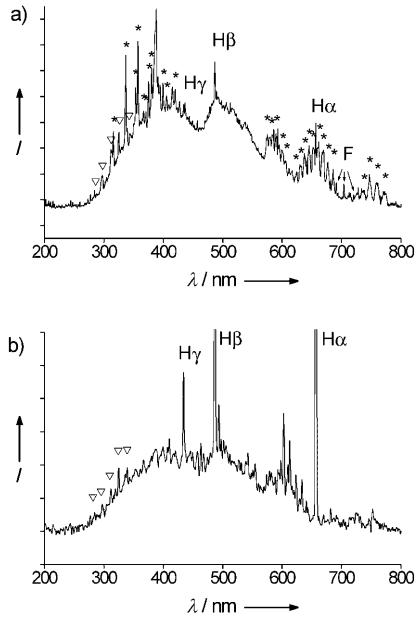

Figure 2. OES data of the plasma (impinging an hBN holder) with a gas flow of a) 5 std $cm^3 min^{-1}$ BF_3 and b) 5 std $cm^3 min^{-1}$ BF_3 and 10 std $cm^3 min^{-1}$ H_2. Emissions from N_2 (*) and BF (▽) are indicated.

clusters; F and BF clusters are expected in the BF_3 plasma. The small quantity of atomic hydrogen evident, which decreased with time, is likely to have arisen from residual H_2 released from the surfaces of the chamber. The signal corresponding to N_2 was constant with time and no N_2 was introduced into the system. The emission intensity of both N_2 and F decreased with the introduction of H_2 and finally disappeared (Figure 2b) for a gas flow rate of 5 std $cm^3 min^{-1}$ for BF_3 and 10 std $cm^3 min^{-1}$ for H_2. The signal corresponding to N_2 that followed a periodic decrease and increase of the H_2 flow rate was studied and observed only for low flow rates of H_2. This observation rules out residual N_2 in the system as the N_2 source. Therefore, the etching of the hBN substrate holder by F atoms, which are formed in pure BF_3 plasma or BF_3 plasma with low H_2 concentrations, is the only plausible source of N_2. The concentration of F atoms decreases with the introduction of H_2 as a result of the formation of HF, which seems not to react with hBN. Hence, the hBN etching (revealed by the N_2 signal) stops at a sufficiently high concentration of H_2. The etching of hBN at only low H_2/BF_3 ratios is in accord with the optimal window of the H_2/BF_3 ratio for successful cBN deposition, whereas at higher H_2/BF_3 ratios only hBN films evolve.[16] The flow rate of H_2 controls the production rate of solid BN from the gas phase, and the ratio of H to F atoms controls the equilibrium between film formation and etching.

The last observation from this OES study is the nearly constant emission intensity of the BF_x cluster with increasing hydrogen flow rates, whereas no signal pertaining to BH_x clusters could be detected. This result suggests that the growth species are clusters of BF_x rather than of BH_x. This finding from OES is consistent with the higher bond energy of the B–F bond (757 kJ mol^{-1}) relative to that of the B–H bond (340 kJ mol^{-1}). Quantum mechanical calculations indicate that B–F termination stabilizes the boron surface of cBN.[17,18] The F-terminated boron surface, however, was found by quantum mechanical calculations to be resistant to abstraction and adsorption of N-containing growth species for further cBN growth.[17,18] B–F bond breaking followed by surface abstraction and adsorption of N-containing species may be facilitated by low-energy ion bombardment, which is still needed for cBN growth from F-containing species.[9,11]

Angle-resolved XPS (VG, EscaLab 220i-XL, $Al_{K\alpha}$ radiation) of cBN films grown by the ECR system was used to gain further insight into the cBN growth process. Spectra were collected at emission angles of 10° and 90° to evaluate the elemental depth distributions, as the probing depth at 90° ($\approx$5 nm) is much larger than that at 10° ($\approx$1 nm).[19] Table 1

Table 1: Elemental concentration calculated from XPS data.

	Elemental Concentration [%]	
Emission angle	90°	10°
B	43.7	39.4
N	47.6	47.7
C	5.7	8.7
O	2.3	3.2
F	0.7	1.0

summarizes the elemental concentration of the film, which includes mainly boron and nitrogen and small amounts of fluorine, carbon, and oxygen. The B/N ratio is less than 1 and decreases from 0.92 to 0.83 with decreasing emission angle (90°→10°) thus indicating boron-deficient surfaces. The low concentration of fluorine (0.7% and 1.0% for 90° and 10°, respectively) indicates that only a small portion of the surface is terminated by F atoms. These results are in accord with the feeding gas composition of the plasma ($BF_3/N_2 = 1.5{:}50$). The high concentration of N_2 in the gas phase leads to a high probability of termination with N atoms. This point was further verified by exposing the film to a $BF_3 + Ar + He$ plasma, which lead to a significant increase of both the B/N ratio (to greater than 1:1) and the concentration of F atoms (to approximately 6%). Further exposure to $N_2 + H_2$ plasma decreased the B/N ratio and the concentration of fluorine to their initial values. Finally, the O and C atoms are mostly surface contaminants from the atmosphere as revealed by the angle-dependent XPS analysis.

We note that N_2 molecules fed to the plasma decompose to N atoms and then combine with H or F atoms. The bonding energies of N–H ($\approx$340 kJ mol^{-1}) and N–F (343 kJ mol^{-1}) are similar,[17,18] so both NH_x and NF_x clusters may exist.

However, the low concentration of F atoms in our present XPS data ($\approx 1\,\%$) rules out the possibility of N–F termination of the cBN surface, and the results of secondary ion mass spectrometry (SIMS) of a cBN film suggest that N atoms are partly bonded to H atoms.[20] It is therefore most likely that only NH_x clusters contribute to the surface processes that lead to cBN growth. Furthermore, we note that the adsorption energy of NH_x clusters ($416\,kJ\,mol^{-1}$) is larger than that of NF_x clusters ($17\,kJ\,mol^{-1}$) on F-terminated boron surfaces.[17,18] N–H bonds are also found to be much more effective than N–F bonds in incorporating B-containing species after H abstraction, and in stabilizing and maintaining sp^3-hybridized surface atoms.[17,18]

Our experimental findings lead to the following conclusions regarding the growth of cBN through the introduction of fluorine-containing species: 1) the growth of cBN is a surface process (HR-TEM data); 2) hBN constituents are etched by F atoms in the plasma (OES data); 3) BF_x and NH_x species are responsible for the growth of cBN (OES and XPS data); 4) the cBN film surface is boron-deficient and the termination of dangling bonds by F atoms is minor (XPS data). On the basis of these conclusions, we now offer the following sequence of cBN growth from fluorine-containing species, as shown in Figure 3:

1) The excited plasma contains reactive species, namely, H, F, BF_x, NH_x, which are responsible for the etching of hBN (mainly F atoms) and cBN crystal growth (BF_x and NH_x) (Figure 3a). The cBN surface at any stage contains a large number of N atoms terminated by H atoms but a very small number of B atoms terminated by F atoms.

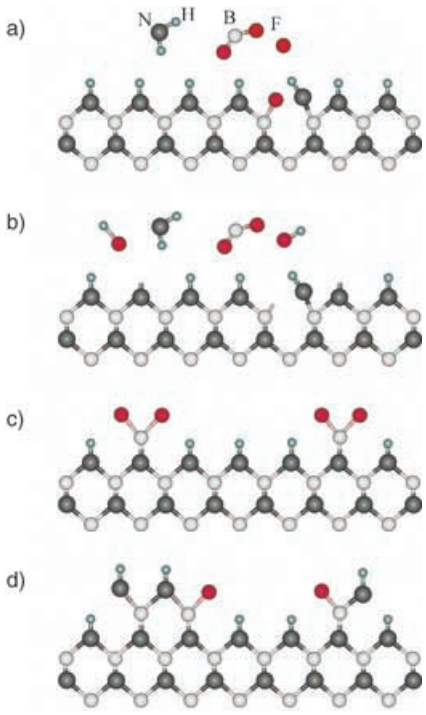

Figure 3. A proposed cBN growth sequence in fluorine-based ECR-assisted MW CVD. The growth is illustrated on a (001) surface (see text for details).

2) The cBN crystal surface is activated by surface abstraction by the impingement of plasma species, thus providing free unsaturated sites for further growth (Figure 3b). B–F bond breaking is most likely assisted by energetic particle bombardment (bias of about 20 V) while N–H bond breaking is easier.
3) B atoms are added to N-activated sites by incorporation of BF_x species, whereas N atoms are added to B-activated sites by incorporation of NH_x species (Figure 3c).
4) Each B surface site is subject to deposition by an NH_x molecule at a much higher rate than the deposition of BF_x on N surface sites (the BF_3/N_2 flow rate feeding the plasma is 1.5:50), thus leading to a B-deficient surface at any stage (Figure 3d).

Layer-by-layer growth of a cBN crystal requires the alternate deposition of B atoms on the nitrogen surface and the deposition of N atoms on the boron surface, which means (on a macroscopic scale) equal surface concentrations of B and N atoms. The surface of our ECR films is B-deficient owing to the plasma composition needed for cBN growth (BF_3/N_2 flow rate = 1.5:50). As stated above, our experimental findings support that N surface atoms are terminated by H atoms, whereas B surface atoms are terminated by F atoms. The N–H bonds of N–H terminated surface sites were found to be energetically effective in abstraction and adsorption of incoming B-containing species.[17,18] The H atom that terminates an N surface atom is abstracted by plasma F atoms to form HF and leave room for BF_x adsorption. The chemical bond strength of B–F is large, which makes it resistant to abstraction and adsorption of NH_x molecules. In our work, the breaking of B–F bonds and formation of a dangling bond needed for NH_x adsorption and further cBN growth are most likely to be facilitated by the low-energy ion bombardment of the growing surface (Figure 3b).

The high abundance of N-containing clusters in the plasma (relative to B-containing clusters) dictates that the coverage rate of each B surface atom (F terminated) by N atoms will be much larger than the coverage rate of N surface atoms (H terminated) by B atoms. This rules out the possibility of a layer-by-layer growth and leaves island formation of cBN with a major surface coverage of H-terminated N atoms as the dominant growth mechanism (Figure 3d). The hydrogen concentration in the plasma determines 1) the concentration of NH_x species (needed for growth) which increases with the concentration of H atoms; 2) the concentration of F atoms (needed for activation of H-terminated N surface atoms and for etching of noncubic BN constituents) which decreases with H concentration. This is how the hydrogen/fluorine ratio controls the deposition rate and phase purity resulting in an optimal window of the H_2/BF_3 ratio for cBN growth.[16]

In conclusion, a combination of HR-TEM, OES, and XPS studies has revealed that ECR fed by a gas mixture of $He(Ar)/N_2/BF_3/H_2$ leads to the surface CVD growth of cBN, which is fundamentally different from PVD growth by ion-assisted methods. The new data collectively support a cBN surface-growth sequence, which includes 1) formation of H, F, BF_x, and NH_x species in the plasma in which the amount of F

and NH_x species is balanced by the concentration of hydrogen atoms, 2) abstraction of H atoms and activation of N sites by F atoms, 3) abstraction of F atoms and activation of B sites by energetic particle bombardment, 4) growth by adsorption of BF_x (boron source) on N surfaces and NH_x (N source) on B surfaces, and 5) etching of noncubic BN phases by F atoms. The possibility to grow cBN through surface reactions with little damage from ion bombardment suggests that the growth of electronic grade, single-crystal cBN wafers is feasible (similar to electronic grade, single-crystal diamond wafers grown by CVD).

Received: January 27, 2005
Revised: April 15, 2005
Published online: July 1, 2005

Keywords: chemical vapor deposition · crystal growth · nitrides · plasma chemistry · reaction mechanisms

[1] R. H. Wentorf, *J. Chem. Phys.* **1962**, *36*, 1990 – 1991.
[2] P. B. Mirkarimi, K. F. McCarty, D. L. Medlin, W. G. Wolfer, T. A. Friedmann, E. J. Klaus, G. F. Cardinale, D. G. Howitt, *J. Mater. Res.* **1994**, *9*, 2925 – 2938.
[3] T. Yoshida, *Diamond Relat. Mater.* **1996**, *5*, 501 – 507, and references therein.
[4] W. J. Zhang, I. Bello, Y. Lifshitz, S. T. Lee, *MRS Bull.* **2003**, *28*, 184 – 188, and references therein.
[5] X. W. Zhang, H. G. Boyen, N. Deyneka, P. Ziemann, F. Banhart, M. Schreck, *Nat. Mater.* **2003**, *2*, 312 – 315.
[6] Y. Lifshitz, S. R. Kasi, J. W. Rabalais, W. Eckstein, *Phys. Rev. B* **1990**, *41*, 10468 – 10480.
[7] Y. Lifshitz, T. Kohler, T. Frauenheim, I. Guzmann, A. Hoffman, R. Q. Zhang, X. T. Zhou, S. T. Lee, *Science* **2002**, *297*, 1531 – 1533.
[8] P. B. Mirkarimi, K. F. McCarty, D. L. Medlin, *Mater. Sci. Eng. R* **1997**, *21*, 47 – 100, and references therein.
[9] W. J. Zhang, S. Matsumoto, *Appl. Phys. A* **2000**, *71*, 469 – 472.
[10] W. J. Zhang, S. Matsumoto, K. Kurashima, Y. Bando, *Diamond Relat. Mater.* **2001**, *10*, 1881 – 1885.
[11] C. Y. Chan, W. J. Zhang, X. M. Meng, K. M. Chan, I. Bello, Y. Lifshitz, S. T. Lee, *Diamond Relat. Mater.* **2003**, *12*, 1162 – 1168.
[12] W. J. Zhang, I. Bello, Y. Lifshitz, K. M. Chan, X. M. Meng, Y. Wu, C. Y. Chan, S. T. Lee, *Adv. Mater.* **2004**, *16*, 1405 – 1408.
[13] W. J. Zhang, C. Y. Chan, K. M. Chan, I. Bello, Y. Lifshitz, S. T. Lee, *Appl. Phys. A* **2003**, *76*, 953 – 955.
[14] Z. F. Zhou, I. Bello, M. K. Lei, K. Y. Li, C. S. Lee, S. T. Lee, *Surf. Coat. Technol.* **2000**, *128*, 334 – 340.
[15] W. J. Zhang, X. Jiang, S. Matsumoto, *Appl. Phys. Lett.* **2001**, *79*, 4530 – 4532.
[16] W. J. Zhang, S. Matsumoto, *Chem. Phys. Lett.* **2000**, *330*, 243 – 248.
[17] K. Larsson, J. O. Carlsson, *J. Phys. Chem. B* **1999**, *103*, 6533 – 6538.
[18] B. Mårlid, K. Larsson, J. O. Carlsson, *Phys. Rev. B* **1999**, *60*, 16065 – 16072.
[19] M. P. Seah, W. A. Dench, *Surf. Interface Anal.* **1979**, *1*, 2 – 11.
[20] X. Jiang, K. Helming, W. J. Zhang, S. Matsumoto, *Chem. Vap. Deposition* **2002**, *8*, 262 – 265.

